6-23-2016

# Biotic Regulation of CO2 Uptake–Climate Responses: Links to Vegetation Properties

H. Wayne Polley
*United States Department of Agriculture*

Anne E. Gibson
*United States Department of Agriculture*

Philip A. Fay
*United States Department of Agriculture*

Brian J. Wilsey
*Iowa State University*, bwilsey@iastate.edu

# Biotic Regulation of CO2 Uptake–Climate Responses: Links to Vegetation Properties

**Abstract**
Identifying the plant traits and patterns of trait distribution in communities that are responsible for biotic regulation of $CO_2$ uptake–climate responses remains a priority for modeling terrestrial C dynamics. We used remotely sensed estimates of gross primary productivity (GPP) from plots planted to different combinations of perennial grassland species in order to determine links between traits and GPP–climate relationships. Climatic variables explained about 50% of the variance in temporal trends in GPP despite large variation in $CO_2$ uptake among seasons, years, and plots of differing composition. GPP was highly correlated with contemporary changes in net radiation (Rn) and precipitation deficit (potential evapotranspiration minus precipitation) but was negatively correlated with precipitation summed over 210 days prior to flux measurements. Plots differed in GPP–Rn and GPP–water (deficit, precipitation) relationships. Accounting for differences in GPP–climate relationships explained an additional 11% of variance in GPP. Plot differences in GPP–Rn and GPP–precipitation slopes were linked to differences in community-level light-use efficiency (GEE*). Plot differences in GPP–deficit slopes were linked to differences in a species abundance-weighted index of specific leaf area (SLA). GEE* and weighted SLA represent vegetation properties that may regulate how $CO_2$ uptake responds to climatic variation in grasslands.

**Keywords**
exotic plant species, Grassland, gross primary productivity, net radiation, normalized difference vegetation index, plant traits, precipitation, specific leaf area



**Comments**
This article is published as Polley, H. Wayne, Anne E. Gibson, Philip A. Fay, and Brian J. Wilsey. "Biotic Regulation of CO2 Uptake–Climate Responses: Links to Vegetation Properties." Ecosystems 19, no. 8 (2016): 1376-1385. doi: 10.1007/s10021-016-0009-8. Posted with permission.

Ecosystems (2016) 19: 1376–1385
DOI: 10.1007/s10021-016-0009-8



# Biotic Regulation of $CO_2$ Uptake–Climate Responses: Links to Vegetation Properties

H. Wayne Polley,[1]* Anne E. Gibson,[1] Philip A. Fay,[1] and Brian J. Wilsey[2]

[1]*Grassland, Soil & Water Research Laboratory, USDA–Agricultural Research Service, Temple, Texas 76502, USA;* [2]*Department of Ecology, Evolution and Organismal Biology, Iowa State University, 251 Bessey Hall, Ames, Iowa 50011, USA*

## Abstract

Identifying the plant traits and patterns of trait distribution in communities that are responsible for biotic regulation of $CO_2$ uptake–climate responses remains a priority for modeling terrestrial C dynamics. We used remotely sensed estimates of gross primary productivity (GPP) from plots planted to different combinations of perennial grassland species in order to determine links between traits and GPP–climate relationships. Climatic variables explained about 50% of the variance in temporal trends in GPP despite large variation in $CO_2$ uptake among seasons, years, and plots of differing composition. GPP was highly correlated with contemporary changes in net radiation (Rn) and precipitation deficit (potential evapotranspiration minus precipitation) but was negatively correlated with precipitation summed over 210 days prior to flux measurements. Plots differed in GPP–Rn and GPP–water (deficit, precipitation) relationships. Accounting for differences in GPP–climate relationships explained an additional 11% of variance in GPP. Plot differences in GPP–Rn and GPP–precipitation slopes were linked to differences in community-level light-use efficiency (GEE*). Plot differences in GPP–deficit slopes were linked to differences in a species abundance-weighted index of specific leaf area (SLA). GEE* and weighted SLA represent vegetation properties that may regulate how $CO_2$ uptake responds to climatic variation in grasslands.

**Key words:** exotic plant species; grassland; gross primary productivity; net radiation; normalized difference vegetation index; plant traits; precipitation; specific leaf area.

## Introduction

Carbon fixation by terrestrial vegetation is regulated by biotic and abiotic drivers, the latter including climatic (that is, meteorological or environmental) variables. Climatic drivers regulate C fluxes at local to regional spatial scales and over temporal scales of seconds to months (Hui and others 2003; Polley and others 2010b). However, the flux–climate correlation varies temporally (Hui and others 2003; Richardson and others 2007; Wu and others 2012) and spatially across gradients in vegetation type or disturbance regime (Polley and others 2008) because of biological variation (Richardson and others 2007; Polley and others 2011; Shao and others 2015), including variation in the values of plant traits that affect C uptake and loss (Ma and others 2011; Musavi and others 2015).

Received 17 December 2015; accepted 1 May 2016;
published online 23 June 2016
**Electronic supplementary material:** The online version of this article (doi:10.1007/s10021-016-0009-8) contains supplementary material, which is available to authorized users.
**Author contributions** HWP conceived the study and analyzed data; AEG, PAF, BJW, and HWP collected data and participated in writing the manuscript.
*Corresponding author; e-mail: wayne.polley@ars.usda.gov

Identifying the patterns of trait distribution in communities and community-level physiological features that are responsible for biotic regulation of $CO_2$ uptake–climate responses remains a priority for modeling C dynamics. Accelerating declines in vegetation diversity and the proliferation of exotic plant species (Wardle and others 2011) lend urgency to the challenge of identifying community-level metrics of C cycling.

Considerable progress has been made in distinguishing readily measurable plant traits, such as specific leaf area (SLA) and plant height, that are correlated with productivity at the ecosystem scale (Garnier and others 2004; Díaz and others 2007; Ma and others 2011), but challenges remain in linking trait variation to $CO_2$ uptake. First, some flux–trait studies lack a climatic component, despite the recognized link between meteorological drivers and C fluxes. Second, attempts to link trait variation or community physiological features to fluxes often are challenged by the temporal mismatch in dynamics of fluxes and community attributes. C fluxes respond to potentially rapid changes in meteorological drivers such as temperature and precipitation by shifting over time scales of seconds to seasons, whereas the distribution of plant traits in communities and community physiological attributes typically change more slowly (Ma and others 2011), over seasonal or longer time scales. A clearer understanding of the role of trait variation and physiological attributes in regulating $CO_2$ fluxes thus may require that we represent fluxes by quantities that integrate processes and their environmental responses (Musavi and others 2015) and align temporal scales of trait variation and flux dynamics.

Musavi and others (2015) defined an 'ecosystem functional property' (EFP) as including the responses of physiological processes, such as $CO_2$ uptake, to environmental drivers. We consider the slope of the response of ecosystem gross primary productivity (GPP) to climatic variation as an EFP that varies over temporal scales comparable to those over which the plant traits that affect ecosystem-level photosynthesis vary. Plant traits are measurable features at the individual organ or organism level (Violle and others 2007). Following Mouillot and others (2011), we use the term 'community functional structure (CFS)' to describe the composition, diversity, and distribution of functional traits in plant communities.

Our overall goal was to identify CFS or community-level physiological features that statistically explain an EFP, the response of gross primary productivity (GPP) to climatic variation over seasonal to interannual temporal scales. We sampled GPP and plant traits in multispecies communities planted to all native or all exotic perennial species in the Maintenance of Exotic versus Native Diversity (MEND) experiment (Wilsey and others 2009, 2011). GPP was measured during growing seasons 5–7 following planting, after plot composition had stabilized (Wilsey and others 2011).

We had two specific goals. The first was to identify primary climatic drivers of GPP and the temporal scale of driver variation that was most highly correlated with GPP dynamics. Grassland C fluxes and production usually are regulated by temperature and precipitation, but changes in functioning can lag changes in drivers (Craine and others 2012; Wang and others 2003; Polley and others 2010a). Our second goal was to determine whether among-plot variation in GPP–climate relationships could be explained by variation in either the CFS of plant traits presumed to influence GPP or a community-level index of photosynthetic light-use efficiency, maximum GPP (or gross ecosystem exchange) normalized for light interception (GEE*; Kergoat and others 2008).

We tested the following predictions: (1) Temporal dynamics in community GPP would correlate more strongly with recent (lag $<$ 1 month) than former (lag $>$ 1 month) values of temperature, light, and evaporative demand. Lag effects were predicted to be minimal because photosynthesis rates respond almost immediately to changes in temperature, light, and evaporative demand. (2) The lag in GPP response to precipitation would exceed that in GPP response to temperature, light, and evaporative demand because of the prolonged period following which significant change in soil water content can influence the processes (for example, biogeochemical cycling, structural and compositional change in canopies and communities) that regulate canopy photosynthesis (for example, Sala and others 2012). (3) Slopes of GPP–climate relationships would correlate positively with either GEE* or abundance-weighted or variance-based metrics of plant traits. An increase in Rn should increase C uptake more in communities with high than low light-use efficiency (LUE), leading to a positive relationship between slopes of GPP–Rn relationships and GEE*. Similarly, variation in SLA has been shown to link positively with productivity or photosynthesis at the ecosystem scale (Garnier and others 2004; Díaz and others 2007; Ma and others 2011).

## Methods

### Field Plots

We sampled plots included in the Maintenance of Exotic vs. Native Diversity (MEND) experiment located in central Texas, USA (Wilsey and others 2009, 2011, 2014). MEND is a two-way factorial experiment [Origin (Native/Exotic) x Irrigation (irrigated during summer/not irrigated)] applied using a randomized block design. Equal-sized seedlings of perennial species were transplanted into 1 × 1 m field plots (72 individuals/$m^2$) in two blocks, one planted in October 2007 and the other planted in March 2008. The species composition of plots was determined by random draw from a pool of 18 native or 18 exotic species with the condition that the relative abundances of functional groups of species ($C_4$ grasses, $C_3$ grasses, legumes, nonleguminous $C_3$ forbs) remain constant across plots. For each random selection of 9 native species, we populated one native and one exotic mixture (=draw), the latter by selecting the exotic species that were most closely phylogenetically related to selected natives. Four draws were included in each of the two blocks. Each draw was replicated within each treatment (origin, irrigation) for a total of 32 mixture plots per block (4 draws × 2 origin treatments × 2 irrigation treatments × 2 replicates). Irrigation was applied by hand during the typically dry period of mid-July to mid-August each year at a rate of 128 mm per month. Irrigation was applied as 8 events per year of 16 mm each beginning in 2008. Volunteer plants were removed by hand. No fertilizer was added. Annual precipitation was 96 and 122% of the 100-year mean (876 mm) in 2012/2014 and 2013, respectively.

### Sampling for GPP and NDVI

GPP was estimated from measurements of NDVI for plots planted as 9-species communities. The spectral signature of reflected radiation was measured over each plot (2012–2014) using an ASD Fieldspec 3 spectroradiometer with a spectral range of 350–2500 nm and spectral resolution of 3 nm at 700 nm (ASD Inc., Boulder, CO, USA). We measured reflectance from directly above each plot (1.71 m height) at each of five equally spaced positions along the plot diagonal, providing a spatial resolution of 0.3 m per measurement (10° FOV). Reflectance was measured on cloudless days within 2 h of solar noon. Measurements were referenced to a barium sulfate panel at c. 15 min intervals. Reflectance was measured at c. monthly intervals in 2012 and biweekly intervals in 2013 and 2014. We averaged the 5 measurements per plot from each day to calculate NDVI:

$$\mathrm{NDVI} = \frac{\mathrm{NIR} - \mathrm{VIS}}{\mathrm{NIR} + \mathrm{VIS}}, \quad (1)$$

where NIR and VIS are reflectance in the near infrared (730–900 nm) and visible spectral ranges (550–680 nm), respectively.

During May, July, and September 2013 and March 2014, we measured both NDVI and rates of $CO_2$ exchange of selected communities. Our goal was to develop a relationship between NDVI and GPP as calculated from $CO_2$ fluxes. Rates of net ecosystem exchange (NEE) were determined by measuring the rate of $CO_2$ depletion in a 0.752-$m^3$ chamber (90 × 91.5 × 91.5 cm) following placement on plots. The chamber is constructed of clear acrylic (OPTIX® Plaskolite, Inc., Columbus, Ohio) with 92% visible light transmittance. The bottom of the chamber was framed with 3.8 cm × 3.8 cm aluminum angle faced with closed cell rubber stripping, which mated with a 5 cm × 5 cm angle iron frame pressed into the soil at least 24 h before measurements.

$CO_2$ and $H_2O$ vapor concentrations in the chamber were measured with an open-path infrared gas analyzer (IRGA; LI-7500A LI-COR Biosciences, Lincoln, NE, USA). The IRGA was calibrated for $CO_2$ using a 350 ppm $CO_2$ certified standard gas, and for $H_2O$ vapor with a dewpoint generator. The chamber contained a quantum sensor (LI-190, LI-COR, Lincoln, Nebraska) to measure the flux of photosynthetically active radiation (PAR), a shielded and aspirated air temperature/relative humidity sensor (LI-COR 1400-104), and eight 120-mm-diameter circulating fans.

NEE was measured under mostly clear skies by placing the chamber on the frame, allowing the chamber air to mix (10–30 s), then recording $CO_2$ change at 1 s intervals for 60–90 s. The chamber was then darkened with a reflective insulation cover (Reflectix®, Markleville, IN, USA), and ecosystem respiration (Re) was measured over the following 60 s. NEE and Re were calculated as per Jasoni and others (2005). Instantaneous ecosystem GPP (μmol $CO_2$ $m^{-2}$ $s^{-1}$) was calculated by subtracting Re from NEE. Positive values denote fluxes toward the surface. Spectral reflectance was measured shortly after NEE was measured.

### Plant Traits, Functional Diversity, and Community Light-Use Efficiency

Aboveground biomass per species in each mixture plot was measured nondestructively in June and

October of each year (2012–2014) using a point intercept technique (Wilsey and others 2011). Regression relationships between the number of intercepts per species and species biomass were used to calculate aboveground biomass per species.

Maximum plant height and the area and fresh and dry mass of selected leaves were measured in June 2014 on plants grown in monocultures using methods suggested by Cornelissen and others (2003). Leaf C and N contents were measured with a C:N analyzer (Elementar vario Max CN, Elementar, Mt. Laurel, NJ, USA or Fisons NA 1500 NCS, Thermo Fisher Scientific, Waltham, MA, USA). We calculated the following traits: (1) SLA, the ratio of leaf area to leaf dry mass; (2) leaf dry matter content (LDMC), the dry mass of a leaf divided by its saturated fresh weight; and (3) leaf C and N concentrations, expressed both per unit of leaf mass and leaf area.

CFS for each community was quantified using two metrics: First, we calculated a community-weighted mean (CWM) for each trait by weighing the trait values of each species by the relative abundance of the species in the community (Grime 1998; Garnier and others 2004). This abundance-weighted index is interpreted as the trait value expected from a random sample of the community (Díaz and Cabido 2001) and is considered the functional identity of the community (Mouillot and others 2011). We also calculated community-weighted means of selected traits by weighing the trait value of each member species, $x_i$, by the relative height ($Ht_i$; 0–1) of the species in the community using the Lambert–Beer law of extinction (Musavi and others 2015):

$$\mathrm{CWM_{strata}} = \sum x_i \times \left(p_i x\, e^{k(1-\mathrm{Ht}_i)}\right), \qquad (2)$$

where $p_i$ is the relative abundance of species $i$ and $k$ is the light extinction coefficient, here assumed to be 0.5. This 'canopy strata weighting' ($CWM_{strata}$) is based on the assumption that $CO_2$ uptake is greatest among leaves located nearest the top of the canopy where light interception is greatest. Aggregate indices were calculated using averages of aboveground biomass measured in June of 2012–2014 for each plot type (=block × origin × irrigation × draw; hereafter, plot). Second, we calculated the functional divergence of trait values within each community (Mouillot and others 2011) using the functional divergence index ($FD_{var}$; Mason and others 2005). $FD_{var}$ was calculated for each trait considered by weighing the variance in the trait value of each member species ($x_i$) by the abundance of each species in the community:

$$\mathrm{FD_{var}} = 2/\pi \arctan(5V) \text{and} V = \sum p_i(\ln x_i - \ln x)^2, \qquad (3)$$

where ln $x$ is the abundance-weighted mean of the ln of species trait values. $FD_{var}$ quantifies the extent of trait overlap among species in a community. $FD_{var}$ values range between 0 and 1.

GEE* was calculated for each year and treatment by normalizing the maximum value of GPP ($GPP_{max}$) by an estimate of the fraction of incident PAR that was absorbed by the canopy ($fPAR_a$) relative to absorption assumed for a closed canopy ($fPAR_c$ = 0.95):

$$\mathrm{GEE*} = \mathrm{GPP_{max}} \times \mathrm{fPAR_c}/\mathrm{fPAR_a}. \qquad (4)$$

The value of $fPAR_a$ for each treatment was calculated as

$$\mathrm{fPAR_a} = 0.95 \times (1 - e(-k \times \mathrm{LAI})), \qquad (5)$$

where k is the radiation extinction coefficient, assumed to be 0.5, and 0.95 is the proportion of intercepted PAR that is absorbed by plants (Polley and others 2011). Leaf area index (LAI) was estimated using a linear regression fit to the relationship between LAI and the enhanced vegetation index (EVI):

$$\mathrm{EVI} = 2.5 \times ((\mathrm{NIR} - \mathrm{Red})/(\mathrm{NIR} + (6 \times \mathrm{Red}) - (7.5 \times \mathrm{Blue}) + 1)), \qquad (6)$$

where NIR, Red, and Blue are reflectance in the near infrared (841–876 nm), red (620–670 nm), and blue (459–479 nm) spectral ranges, respectively. LAI was positively correlated with EVI for MEND plots (LAI = −1.01 + 6.74 x EVI; adj. $r^2$ = 0.68, $P < 0.0001$).

## Climatic Variables and GPP–Climate Relationships

We summed precipitation (ppt) and calculated means of other climatic variables, including air temperature (AT), vapor pressure deficit of air (vpd), net radiation (Rn), and precipitation deficit (deficit; evaporative demand not met by precipitation), over particular time intervals in order to investigate potential lag effects of climatic variables on GPP. Climatic data were derived from a weather station operated by the Grassland, Soil & Water Research Laboratory (USDA/ARS) and located approximately 1.5 km away from the field site.

Climatic means or sums were calculated over the 90-day period preceding each NDVI measurement. Climatic values were calculated for all possible time

**Table 1.** The Duration and Time Intervals in Days Preceding Each Estimate of GPP Over which AT, vpd, Rn, Deficit, and Related Metrics were Averaged and Precipitation was Summed

| Duration (d) | Time interval (d) | | | | | |
|---|---|---|---|---|---|---|
| 15 | 1–15 | 16–30 | 31–45 | 46–60 | 61–75 | 76–90 |
| 30 | 1–30 | 16–45 | 31–60 | 46–75 | 61–90 | – |
| 45 | 1–45 | 16–60 | 31–75 | 46–90 | – | – |
| 60 | 1–60 | 16–75 | 31–90 | – | – | – |
| 75 | 1–75 | 16–90 | – | – | – | – |
| 90 | 1–90 | – | – | – | – | – |

*See Table 2 for a listing of climate variable abbreviations.*

**Table 2.** Climatic Variables that were Correlated with Variation in Gross Primary Productivity of Grassland Plots Over 3 Years and the Time Interval Prior to Flux Estimates Over which the Correlation of Each Environmental Variable with GPP was Greatest

| Variable | Symbol | Time interval (days) |
|---|---|---|
| Air temperature | AT | 1–15 |
| Long-term precipitation | ppt210 | 1–210 |
| Net radiation | Rn | 16–30 |
| Precipitation | ppt | 16–30 |
| Precipitation deficit | Deficit (=PET−ppt) | 16–30 |
| Vapor pressure deficit | vpd | 1–15 |

*PET potential evapotranspiration.*
*Precipitation was summed and other variables were averaged over each time interval.*

intervals with a minimum duration of 15 days, maximum duration of 90 days, and lag periods of 0, 15, 30, 45, 60, and 75 days (Table 1; $n = 21$ periods). We chose a maximum 75-day lag period for ecosystem response to climate trends as inclusive of most response lags to temperature and precipitation that have been reported (Wang and others 2003; Li and Guo 2012; Wu and others 2015). The time interval for which the sum or mean of each climatic variable best predicted GPP was identified using data pooled from all plots and all 3 years of measurements. GPP also was regressed against precipitation summed over the preceding 7- to 12-month period (for example, days 1–210 and 1–360 prior) because previous year precipitation can affect current year productivity (Sala and others 2012).

Multiple linear regression analysis was used to determine relationships between GPP and climatic variables. In developing regression models, we used values of each climatic variable from the lag period for which the Pearson correlation coefficient ($r$) of the bivariate GPP–climate regression was greatest (Table 2). Trends in three climatic variables, Rn, vpd, and AT, were highly correlated. To better evaluate the independent contributions of Rn, vpd, and AT to GPP, we retained the GPP–Rn regression, replaced vpd with the residuals from a linear regression of vpd on Rn, and replaced AT with the residuals from a linear regression of AT on Rn and the vpd residuals (Graham 2003). We assigned Rn priority over the shared contributions of these variables to GPP change because of evidence that 'light' availability assumes primacy over temperature as a regulator of GPP (Huryn and others 2014). Akaike's Information Criteria (AIC) and Schwarz Bayesian Criteria (SBC) were used to select the multiple regression model that 'best' predicted GPP from among the set of all possible models. Models of greater complexity were chosen when inclusion of an additional model parameter reduced AIC by more than 2 (Burnham and Anderson 2002).

Plots differed in GPP–climate responses partly because they differed in GEE* or in the CFS of traits that regulate $CO_2$ uptake, here termed the biotic effect. Climatic variables retained in multiple regression models with GPP when data from all years and plots were considered were entered into a separate-slopes model (for example, Hui and others 2003). A biotic effect was detected when the slope of one or more of the GPP–climate relationships differed significantly among plots ($n = 32$). Bivariate regression was used to determine contributions of GEE* and the CWM or $FD_{var}$ of traits to variation in GPP–climate slopes.

Structural equation modeling (SEM) was used to assess direct and indirect effects of CFS on slopes of GPP–climate relationships. The SEM model was fit using IBM SPSS AMOS 21 software. The hypothesized relationship among variables in a SEM is considered to be consistent with data when the probability level of the $\chi^2$ statistic is greater than a significance level of $P = 0.05$ (Shipley 2000).

## Results

### Temporal Trends in GPP

Instantaneous rates of GPP were strongly correlated with simultaneously measured values of NDVI [GPP ($\mu$mol $CO_2$ $m^{-2}$ $s^{-1}$) = 1.099 × $e^{(-5.244 \times NDVI)}$; adj. $r^2 = 0.82$, $P < 0.0001$, $n = 115$; not shown]. The EVI explained a lesser fraction of variance in GPP than did NDVI (adj. $r^2 = 0.73$).

NDVI-derived estimates of GPP varied substantially both within and among years and plots, the

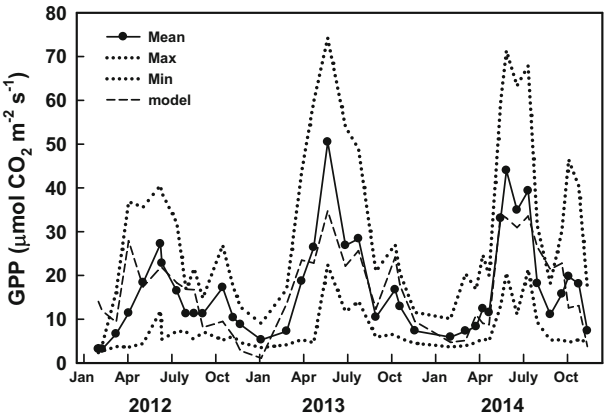


**Figure 1.** Gross primary productivity (GPP) as derived from NDVI measurements for grassland plots. *Solid line* indicates temporal trends in mean values of GPP ($n$ = 32). *Dashed line* indicates trends in GPP as calculated from a multiple regression model fit to climatic variables. *Dotted lines* indicate maximum and minimum values of GPP for each sampling date.

latter evident in large differences between maximum and minimum values of GPP on a given date (Figure 1). GPP followed a bimodal seasonal trend with a large peak in June and smaller peak in late October each year. The bimodal trend was best expressed in years 2012 and 2014 when GPP increased in autumn by approximately 50–75% from minimum values measured during late summer (mid-August through mid-September). Interannual and among-plot variation in GPP also were substantial. Maximum GPP in 2012 was approximately 60–75% of the maximum measured in 2013 and 2014, respectively. Maximum values of GPP were a factor of 3 greater than minimum values during peak C uptake each year.

## GPP–Climate Relationships

A 5-parameter multiple regression model with climatic variables (Table 2) explained 48% of the variance (adj. $r^2$) in plot GPP (Table 3, $P < 0.001$, $n$ = 1152; Figure 1). GPP was positively correlated with Rn (16–30 d) and negatively correlated with variance in AT not explained by Rn (AT residuals; 1–15 d), ppt and deficit (16–30d), and ppt210.

Each of the five climatic variables included in the multiple regression analysis was retained in a model in which slopes of GPP–environment relationships were allowed to vary among plots. Slopes of regression relationships between GPP and three climatic variables (Rn, deficit, ppt210) differed significantly among plots, indicating that variability in GPP was explained partly by factors associated with plot differences in species composition or relative abundances (Table 3). This biotic effect explained 11% of variance in GPP and increased the adj. $r^2$ of the multiple regression model from 0.48 to 0.59.

## Links between the Biotic Effect and Vegetation Properties

Slopes of GPP–deficit regressions were negatively correlated to a community-weighted index of SLA (Figure 2) and the 3-year average of $GPP_{max}$ (adj. $r^2$ = 0.31, $P$ = 0.0006, $n$ = 32) but were positively correlated to weighted N content per unit of leaf area (specific leaf N, SLN; g N $m^{-2}$) [adj. $r^2$ = 0.29, $P$ = 0.0009]. Weighted SLA values were smaller (Figure 2), whereas SLN values were greater on average in native than exotic communities (not shown). Structural equation modeling revealed that variation in GPP–deficit slopes was regulated

**Table 3.** An Analysis of Variance for a Separate-Slopes Regression Model of Temporal Trends in Gross Primary Productivity (GPP; μmol $CO_2$ $m^{-2}$ $s^{-1}$) Over 3 Years for Plots of Perennial Grassland Species ($n$ = 32)

| Variable | Coefficient | Df | Type 1 SS | $F$ | $P$ |
|---|---|---|---|---|---|
| Rn (kJ $m^{-2}$ $d^{-1}$) | $2.157 \times 10^{-3}$ | 1 | 52,633 | 651.9 | <0.0001 |
| deficit (mm $d^{-1}$) | −6.794 | 1 | 21,413 | 265.2 | <0.0001 |
| ppt210 (mm) | $-3.68 \times 10^{-2}$ | 1 | 16,323 | 202.2 | <0.0001 |
| AT residuals (°C) | −1.743 | 1 | 6831 | 84.6 | <0.0001 |
| ppt (mm) | −0.381 | 1 | 4300 | 53.3 | <0.0001 |
| Rn × plot | – | 31 | 14,095 | 5.6 | <0.0001 |
| ppt210 × plot | – | 31 | 4781 | 1.9 | 0.002 |
| deficit × plot | – | 31 | 4318 | 1.7 | 0.009 |
| Error | – | 1053 | 85,019 | – | – |
| Total | – | 1151 | 209,713 | – | – |

*Also listed is the regression coefficient for each variable. See Table 2 for a listing of variable abbreviations.*

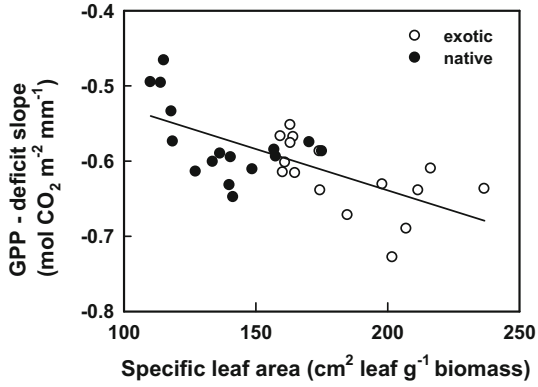


**Figure 2.** Slopes of the regression relationship between gross primary productivity and precipitation deficit (GPP–deficit) over three seasons varied as a negative function of the abundance-weighted mean of specific leaf area (SLA) of grassland plots of differing composition. The line is a linear regression fit to the relationship between GPP–deficit slopes and SLA (adj. $r^2 = 0.42$, $P < 0.0001$, $n = 32$). Different symbols are used to denote data from plots planted to all exotic vs all native species.

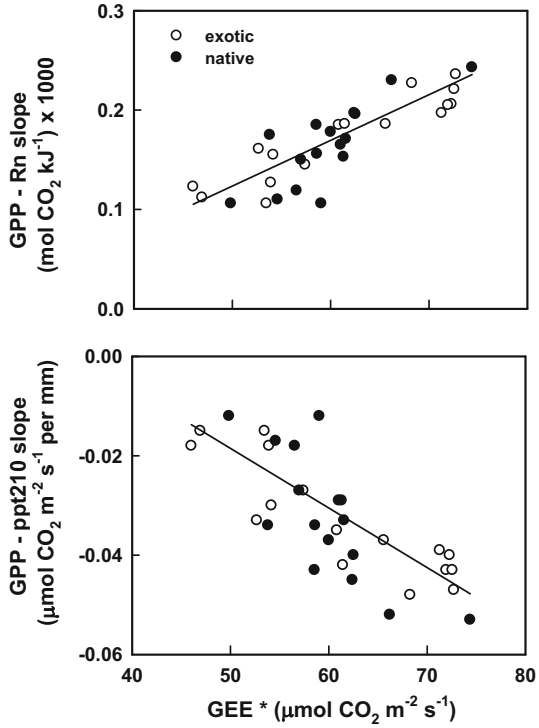


**Figure 3.** Slopes of regression relationships between gross primary productivity (GPP) and both net radiation (Rn; *upper panel*) and precipitation summed over 210 d prior to flux measurements (ppt210; *lower panel*) varied as a function of the seasonal maximum GPP normalized by canopy light absorption (GEE*) of grassland plots of differing composition. Lines are linear regression fits to the relationship between GPP–Rn or GPP–ppt210 slopes and GEE*, a proxy for light-use efficiency (adj. $r^2 = 0.71$ and 0.60, respectively, $P < 0.0001$, $n = 32$). *Different symbols* denote data from plots planted to all exotic vs all native species

by weighted SLA via both a direct pathway (standardized path coefficient, $p_{SLA} = -0.34$) and indirect pathways through weighted SLN (standardized path coefficient, $p_{SLA\_SLN} = 0.16$) and $GPP_{max}$ (standardized path coefficient, $p_{SLA\_GPPmas} = -0.17$) [supplemental Figure 1]. Greater SLA increased the amount by which a given rise in deficit reduced GPP partly by increasing $GPP_{max}$ and reducing SLN.

By contrast, we found no link between the GPP response to Rn or precipitation and either the CWM or $FD_{var}$ of plant traits. Rather, GPP–Rn and GPP–ppt210 slopes varied as function of GEE* (Figure 3). GPP increased more per unit of increase in Rn in communities with high than low GEE*. On the other hand, slopes of regressions between GPP and ppt210 were more negative among communities with high than low values of GEE*. GPP–Rn and GPP–ppt210 slopes were similar among exotic and native communities.

## Discussion

Climatic variables explained about 50% of the variance in temporal trends in grassland GPP despite large variation in $CO_2$ uptake among seasons, years, and plots of differing species composition. GPP was highly correlated with contemporary changes in Rn and precipitation deficit, consistent with our prediction that photosynthetic rates would respond rapidly to changes in these climatic variables. Unexpectedly, however, GPP was negatively correlated with precipitation summed over 210 days prior to flux measurements. Plots differed in two EFPs, the slopes of GPP–Rn and GPP–water (precipitation, deficit) regressions. Consistent with our prediction, EFPs varied among plots because of variation in either GEE* or an abundance-weighted metric of SLA. Plot differences in GPP–Rn and GPP–precipitation slopes were linked to differences in GEE*, a proxy for LUE. Plot differences in GPP–deficit slopes were negatively correlated to weighted SLA. GEE* and weighted SLA represent vegetation properties that contributed to biotic regulation of grassland GPP.

GPP of the grassland communities we studied was correlated with contemporary changes in both Rn and deficit. The GPP–Rn relationship was positive, as anticipated if PAR is a positive function of Rn as observed for a grassland ecosystem (Polley and others 2010a). Conversely, the GPP–deficit relationship was negative, likely a reflection of

photosynthetic sensitivity to excessive evaporative demand. Net $CO_2$ exchange was regulated by precipitation and deficit for desert sites, but by Rn and AT for Great Plains grasslands (Polley and others 2010a).

GPP responded more to cumulative (7 months) than contemporary precipitation and declined rather than rose as precipitation increased. Flux and remote sensing studies of grassland/rangeland ecosystems generally report a positive correlation between precipitation and both $CO_2$ uptake and surrogates for uptake (NDVI, EVI) [Wang and others 2003; Li and Guo 2012; Moran and others 2014; Wagle and others 2015], with the strength of $CO_2$ uptake–precipitation relationships dependent on the time period over which precipitation is considered. GPP or production responses to precipitation have been shown to lag water input or depend more on cumulative precipitation over a given time period than on contemporary water input (for example, Sala and others 2012). NDVI–precipitation correlations for Great Plains grassland were positive and strongest when calculated using precipitation received during the 4–8 weeks prior to NDVI measurement, for example (Wang and others 2003). Lags in photosynthetic responses to precipitation result from slowly manifest changes in canopy development and physiology (Sala and others 2012). The cumulative total of antecedent precipitation may be an especially strong regulator of GPP following periods during which the pool of available soil water has been depleted. Annual precipitation was greater than or equal to the long-term mean for the site during the 3 years of measurements but was only 41% of the mean for the site during 2011, the year prior to measurements. Depletion of soil water during the 2011 drought may have contributed to the link between cumulative precipitation and GPP that we observed in subsequent years.

Per unit of increase in Rn, GPP increased more when GEE* was high than low. One common formulation of the LUE model of canopy photosynthesis equates GPP to the product of incident PAR, which is positively correlated to Rn at a given site, $fPAR_a$, and C uptake per unit of absorbed PAR (Gamon 2015). According to this model, the GPP of communities exposed to the same PAR should increase as GEE* or LUE increases provided that $fPAR_a$ is similar among communities. Of the two variables in the calculation of GEE* that differed among communities (Eq. 4; $GPP_{max}$, $fPAR_a$), $fPAR_a$ varied the least. The $fPAR_a$ varied by a maximum of 30% (from 0.59 to 0.77) among plots, whereas $GPP_{max}$ varied by almost a factor of 2 among plots (from 30.9 to 59.3 μmol $CO_2$ $m^{-2}$ $s^{-1}$). The GPP–Rn response scaled positively with GEE* because communities absorbed a similar fraction of light.

GPP decreased as ppt210 increased, particularly in communities with high GEE*. High GPP should increase litter input and, over several years, litter accumulation. Enhanced litter accumulation could, in turn, suppress the sensitivity of C uptake to precipitation. As GEE* was positively correlated to GPP, enhanced litter accumulation could lead to more negative GPP–ppt210 slopes in communities with high than low GEE*.

GPP declined more per unit of increase in precipitation deficit in communities with canopies of relatively thin than thick leaves (high than low SLA). High values of SLA often are associated with rapid growth of plants and plant communities (Reich and others 1997; Garnier and others 2004), as they were with $GPP_{max}$ in our data. The greater is the growth, the greater, likely, will be the absolute decline in C uptake when evaporative demand exceeds water availability or soil water availability declines (Pfisterer and Schmid 2002; Maseda and Fernández 2015).

Temporal trends in GPP were correlated with temporal trends in climate in grassland plots that differed in species composition. The imprint of species composition on $CO_2$ uptake was evident in plot differences in the GPP response to Rn and water variables, which in turn were linked to stand-level differences in GEE* and weighted SLA. Interestingly plot differences in slopes of GPP–Rn and GPP–deficit/precipitation regressions were correlated (adj. $r^2 = 0.33–0.95$), implying that compositional effects on GPP–climate responses were regulated by a comparably small set of interrelated plant traits. We posit that GEE* and community-weighted SLA represent vegetation functional properties (Musavi and others 2015) that can be measured in situ or, potentially, via remote sensing to improve our capacity to predict biotic effects on $CO_2$ uptake by grassland ecosystems.

## ACKNOWLEDGEMENTS

Field and laboratory assistance from Katherine Jones and Chris Kolodziejczyk was invaluable. This work was partially funded by the USDA-NIFA via Grant 2014-67003-22067. Mention of trade names or commercial products does not imply endorsement by the US Department of Agriculture. USDA is an equal opportunity provider and employer.

## REFERENCES


Burnham KP, Anderson DR. 2002. Model selection and multimodel inference—a practical information-theoretic approach. 2nd edn. New York: Springer, p 488

Cornelissen JHC, Lavorel S, Garnier E, Díaz S, Buchmann N, Gurvich DE, Reich PB, ter Steege H, Morgan HD, van der Heijden MGA, Pausas JG, Poorter H. 2003. A handbook of protocols for standardized and easy measurement of plant functional traits worldwide. Aust J Bot 51:335–380

Craine JM, Nippert JB, Elmore AJ, Skibbe AM, Hutchinson SL, Brunsell NA. 2012. Timing of climate variability and grassland productivity. Proc Natl Acad Sci USA 109:3401–3405

Díaz S, Cabido M. 2001. Vive la difference: plant functional diversity matters to ecosystem processes. Trends Ecol Evol 16:646–655

Díaz S, Lavorel S, de Bello F, Quétier F, Grigulis K, Robson TM. 2007. Incorporating plant functional diversity effects in ecosystem service assessments. Proc Natl Acad Sci USA 104:20684–20689

Gamon JA. 2015. Reviews and syntheses: optical sampling of the flux tower footprint. Biogeosciences 12:4509–4523

Garnier E, Cortez J, Billes G, Navas ML, Roumet C, Debussche M, Laurent G, Blanchard A, Aubry D, Bellmann A, Neill C, Toussaint JP. 2004. Plant functional markers capture ecosystem properties during secondary succession. Ecology 85:2630–2637

Graham MH. 2003. Confronting multicollinearity in ecological multiple regression. Ecology 84:2809–2815

Grime JP. 1998. Benefits of plant diversity to ecosystems: immediate, filter and founder effects. J Ecol 86:902–910

Hui D, Luo Y, Katul G. 2003. Partitioning interannual variability in net ecosystem exchange between climatic variability and functional change. Tree Physiol 23:433–442

Huryn AD, Benstead JP, Parker SM. 2014. Seasonal changes in light availability modify the temperature dependence of ecosystem metabolism in an arctic stream. Ecology 95:2826–2839

Jasoni RL, Smith SD, Arnone JA III. 2005. Net ecosystem $CO_2$ exchange in Mojave Desert shrublands during the eighth year of exposure to elevated $CO_2$. Glob Change Biol 11:749–756

Kergoat L, Lafont S, Arneth A, Le Dantec V. 2008. Nitrogen controls plant canopy light-use efficiency in temperate and boreal ecosystems. J Geophys Res 113(G04017):2008. doi:10.1029/2007/JG000676

Li Z, Guo X. 2012. Detecting climate effects on vegetation in northern mixed prairie using NOAA AVHRR 1-km time-series NDVI data. Remote Sens 4:120–134

Ma S, Baldocchi DD, Mambelli S, Dawson TE. 2011. Are temporal variations of leaf traits responsible for seasonal and inter-annual variability in ecosystem $CO_2$ exchange? Funct Ecol 25:258–270

Maseda PH, Fernández RJ. 2015. Growth potential limits drought morphological plasticity in seedlings from six Eucalyptus provenances. Tree Physiol 36:243–251

Mason NWH, Mouillot D, Lee WG, Wilson JB. 2005. Functional richness, functional evenness and functional divergence: the primary components of functional diversity. Oikos 111:112–118

Moran MS, Ponce-Campos GE, Huete A, McClaran MP, Zhang Y, Hamerlynck EP, Augustine DJ, Gunter SA, Kitchen SG, Peters DPC, Starks PJ, Hernandez M. 2014. Functional response of U.S. grasslands to the early 21st-century drought. Ecology 95:2121–2133

Mouillot D, Villéger S, Scherer-Lorenzen Mason NWH. 2011. Functional structure of biological communities predicts ecosystem multifunctionality. PLoS ONE 6:e17476

Musavi T, Mahecha MD, Migliavacca M, Reichstein M, van de Weg MJ, van Bodegom PM, Bahn M, Wirth C, Reich PB, Schrodt F, Kattge J. 2015. The imprint of plants on ecosystem functioning: a data-driven approach. Int J Appl Earth Obs Geoinf 43:119–131

Polley HW, Emmerich W, Bradford JA, Sims PL, Johnson DA, Saliendra NZ, Svejcar T, Angell R, Frank AB, Phillips RL, Snyder KA, Morgan JA. 2010. Physiological and environmental regulation of interannual variability in $CO_2$ exchange of rangelands in the western United States. Glob Change Biol 16:990–1002

Polley HW, Emmerich W, Bradford JA, Sims PL, Johnson DA, Saliendra NZ, Svejcar T, Angell R, Frank AB, Phillips RL, Snyder KA, Morgan JA, Sanabria J, Mielnick PC, Dugas WA. 2010. Precipitation regulates the response of net ecosystem $CO_2$ exchange to environmental variation on United States rangelands. Rangel Ecol and Manag 63:176–186

Polley HW, Frank AB, Sanabria J, Phillips RL. 2008. Interannual variability in carbon dioxide fluxes and flux-climate relationships on grazed and ungrazed northern mixed-grass prairie. Glob Change Biol 14:1620–1632

Polley HW, Phillips RL, Frank AB, Bradford JA, Sims PL, Morgan JA, Kiniry JR. 2011. Variability in light-use efficiency for gross primary productivity on Great Plains grasslands. Ecosystems 14:15–27

Pfisterer AB, Schmid B. 2002. Diversity-dependent production can decrease the stability of ecosystem functioning. Nature 416:84–86

Reich PB, Walters MG, Ellsworth DS. 1997. From tropics to tundra: global convergence in plant functioning. Proc Natl Acad Sci (USA) 94:13730–13734

Richardson AD, Hollinger DY, Aber JD, Ollinger SV, Braswell BH. 2007. Environmental variation is directly responsible for short- but not long-term variation in forest–atmosphere carbon exchange. Glob Change Biol 13:788–803

Sala OE, Gherardi LA, Reichmann L, Jobbágy E, Peters D. 2012. Legacies of precipitation fluctuations on primary production: theory and data synthesis. Philos Trans R Soc B 367:3135–3144

Shao J, Zhou X, Luo Y, Li B, Aurela M, Billesbach D, Blanken PD, Bracho R, Chen J, Fischer M, Fu Y, Gu L, Han S, He Y, Kolb T, Li Y, Nagy Z, Niu S, Oechel WC, Pinter K, Shi P, Suyker A, Torn M, Varlagin A, Wang H, Yan J, Yu G, Zhang J. 2015. Biotic and climatic controls on interannual variability in carbon fluxes across terrestrial ecosystems. Agric For Meteorol 205:11–22

Shipley B. 2000. Cause and correlation in biology: a user's guide to path analysis, structural equations and causal inference. Cambridge: Cambridge University Press, p 317p

Violle C, Navas M-L, Vile D, Kazakou E, Fortunel C, Hummel I, Garnier E. 2007. Let the concept of trait be functional!. Oikos 116:882–892

Wagle P, Xiao X, Scott RL, Kolb TE, Cook DR, Brunsell N, Baldocchi DD, Basara J, Matamala R, Zhou Y, Bajgain R. 2015. Biophysical controls on carbon and water vapor fluxes across a grassland climatic gradient in the United States. Agric For Meteorol 214–215:293–305

Wang J, Rich PM, Price KP. 2003. Temporal responses of NDVI to precipitation and temperature in the central Great Plains, USA. Int J Remote Sens 24:2345–2364

Wardle DA, Bardgett RD, Callaway RM, Van der Putten WH. 2011. Terrestrial ecosystem responses to species gains and losses. Science 332:1273–1277

Wilsey BJ, Daneshgar PP, Hofmockel K, Polley HW. 2014. Invaded grassland communities have altered stability-maintenance mechanisms but equal stability compared to native communities. Ecol Lett 17:92–100

Wilsey BJ, Daneshgar PP, Polley HW. 2011. Biodiversity, phenology and temporal niche differences between native- and novel exotic-dominated grasslands. Perspect Plant Ecol Evol Syst 13:265–276

Wilsey BJ, Teaschner TB, Daneshgar PP, Isbell FI, Polley HW. 2009. Biodiversity maintenance mechanisms differ between native and novel exotic-dominated communities. Ecol Lett 12:432–442

Wu D, Zhao X, Liang S, Zhou T, Huang K, Tang B, Zhao W. 2015. Time-lag effects of global vegetation responses to climate change. Glob Change Biol 21:3520–3531

Wu J, van der Linden L, Lasslop G, Carvalhais N, Pilegaard K, Beier C, Ibrom A. 2012. Effects of climate variability and functional changes on the interannual variation of the carbon balance in a temperate deciduous forest. Biogeosciences 9:13–28